Types of Renormalization Group Flows

In these notes I solve the renormalization group equations (RGE) and explore the ways the running couplings $g(E)$, $\lambda(E)$, and/or $\alpha(E)$ of different theories change with the energy scale E. For simplicity, I focus mostly on theories with a single coupling — which I call g regardless of its type — and explore its energy dependence for different types of beta-functions. But in the last section of these notes I explore the RG flows in the two-coupling Yukawa theory and generalize to other kinds of multi-coupling theories.

RG Flow for $\beta > 0$

Consider a QFT with a single coupling g, and suppose it has a positive beta-function $\beta(g) > 0$ for all g, weak or strong. Consequently, the running coupling $g(E)$ monotonically increases with energy. But what is the manner of this increase? In particular, given $g(E_1) = E_1$ at some fixed energy E_1, how does $g(E_2)$ behave at much higher energies $E_2 \to \infty$?

Formally solving the renormalization group equation

$$\frac{dg(E)}{d\log E} = \beta(g(E)), \tag{1}$$

we get

$$\int\limits_{g(E_1)}^{g(E_2)} \frac{dg}{\beta(g)} = \log\frac{E_2}{E_1}\,, \tag{2}$$

so the manner in which $g(E_2)$ rises with the E_2 depends on the behavior of $\beta(g)$ at large g.

(A) Suppose at large g, $\beta(g)$ increases faster than $g^{1+\epsilon}$,

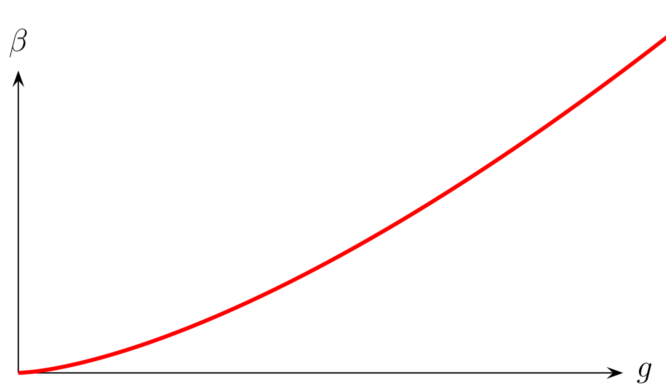

(3)

In this case, the integral

$$I \stackrel{\text{def}}{=} \int_{g_1}^{\infty} \frac{dg}{\beta(g)} \quad \text{is finite.} \tag{4}$$

Consequently, according to eq. (2), $g(E_2)$ reaches infinity for a

$$\text{finite } \log\frac{E_2}{E_1} = I \quad\Longrightarrow\quad \text{finite } E_2 = E_1 \times \exp(I), \tag{5}$$

thus

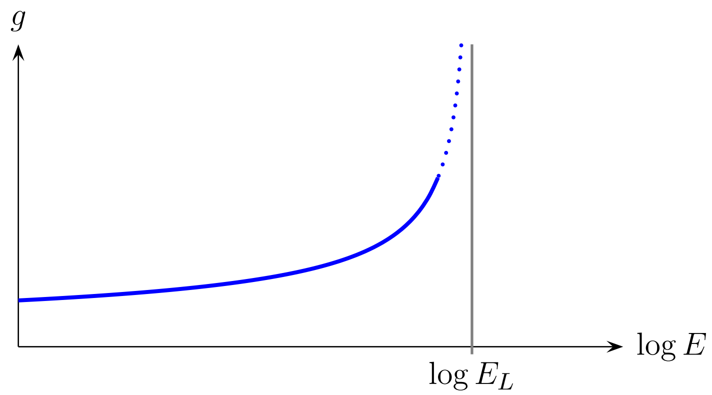

(6)

The energy $E_L = E_1 \times e^I$ at which the coupling blows up is called the *Landau pole*, after speculation by Lev Landau as to what would happen to the QED coupling $e(E)$ at ultra-high energies assuming the one-loop beta-function $\beta(e) = +e^3/12\pi^2$ persists at strong e. Similar to QED, the $\lambda\Phi^4$ theory — in the one-loop approximation to its beta-function — also has a Landau pole at some very high energy scale.

(B) Now suppose the $\beta(g)$ does not increase with large g, or increases no faster than g^1,

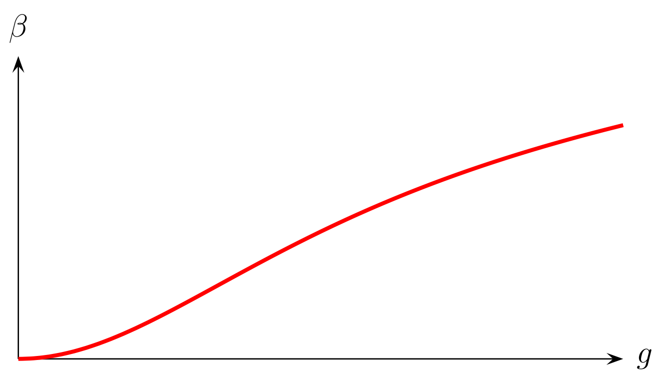

(7)

In this case, the integral

$$I \stackrel{\text{def}}{=} \int\limits_{g_1}^{\infty} \frac{dg}{\beta(g)} \quad \text{is infinite.} \tag{8}$$

In this case, eq. (2) tells us that $g(E_2)$ does not reach ∞ for any finite E_2, so there is no Landau pole. Instead, at very high E_2, $g(E_2)$ becomes large and keeps growing as the energy keeps increasing, but it stays finite at all finite energies:

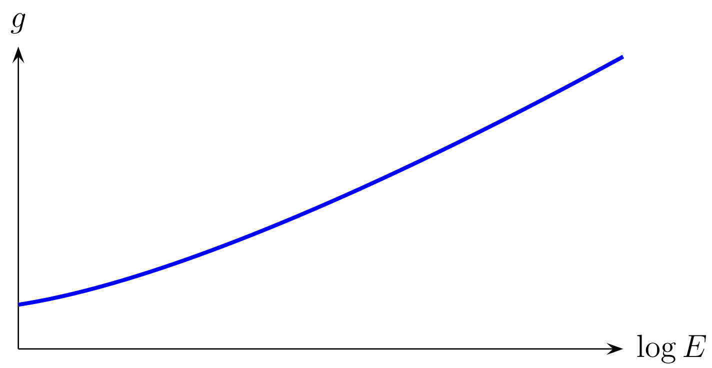

(9)

Alas, in perturbation theory we are limited to calculating $\beta(g)$ at weak $g \ll 1$, but we may only speculate how $\beta(g)$ behaves at strong $g \gg 1$. Consequently, we don't know if the theory has an actual Landau pole where the coupling blows up at some high but finite energy. What we can do is to work out the renormalization group flow of the running coupling $g(E)$ for as long as it stays perturbatively weak, and to estimate the limiting energy E_{lim} at which the coupling $g(E_{\text{lim}})$ becomes too strong for the perturbation theory. But beyond E_{lim}, the perturbation theory breaks down, and we need a different theory to describe the physics at higher energies. Consequently, *the original QFT is not a UV-complete theory but only an effective theory for energies $E \lesssim E_{\text{lim}}$*.

As to the physics at energies $E \gtrsim E_{\text{lim}}$, it could be described by a different QFT with with more or different fields than the low energy theory. Or it could be a very different kind of a theory: maybe a theory of discrete degrees of freedom on some kind of a 4D lattice, maybe a string theory, or maybe something radically different we have not invented yet. But it cannot be the original perturbative low-energy QFT.

⋆ ⋆ ⋆

To complete this section, let switch directions of the RG flow from the UV limit of very high energies to the IR limit of very low energies. In this limit, the coupling $g(E)$ remains perturbatively weak, and its specific behavior at $E \to 0$ depends on masses rather than on the details of the $\beta(g)$:

- If all the particles of the theory are massive — or if the theory without its massive particles becomes free, — then the RG flow stops for $E \lesssim M$ and the running coupling becomes constant,

$$g(E) \;\to\; g_0 \quad \text{for} \quad E \ll M. \tag{10}$$

  For example, in QED the running of the $\alpha(E)$ stops for $E \ll$ Mass of the lightest charged particle, the electron, because at $E \ll M_e$ the EM fields become effectively free.

⋆ But if the theory has massless particles with non-trivial interactions among themselves, then the RG flow continues all the way to $E \to 0$. In this case, $g(E)$ keeps becoming weaker and weaker with lower and lower energies, and ultimately — for the exponentially low energies and exponentially long distances — $g(E)$ becomes so weak the deep-IR theory is almost free.

RG Flow for $\beta < 0$: Asymptotic Freedom

For a negative $\beta(g)$, the running coupling decreases with the energy scale E:

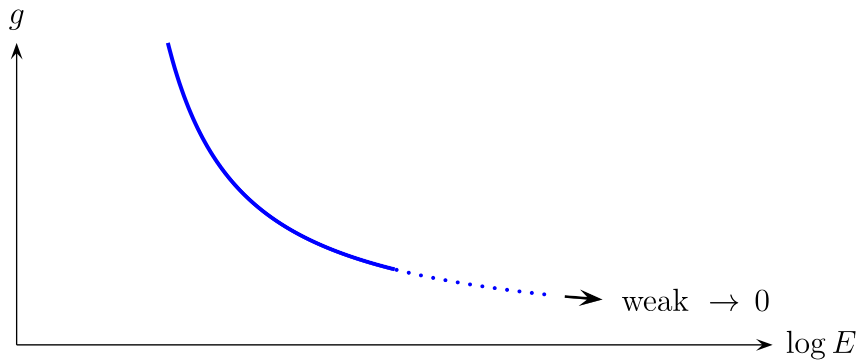

(11)

For high enough energies, $g(E)$ becomes so weak that the theory is almost free and the fields' quanta behave as almost free particles. This is known as the *asymptotic freedom*, where the 'asymptotic' refers to $E \to \infty$ limit, or equivalently distance $\to 0$.

Experimentally, the strong interactions were discovered to be asymptotically free in 1968 at the Stanford Linear Accelerator Center (SLAC). Friedman, Kendall, Taylor, *et al* were studying deep inelastic scattering of electrons by protons; by *deep* inelastic, it means the initial proton turns into may hadrons in the final state. From this scattering they obtained the so-called structure functions of the initial-state proton; although these structure functions are different from the on-shell form factors we have studied in this class, they also help us understand how the electric charge and the magnetic moment are distributed across the proton, and with much higher spatial resolution. To everybody's surprise, Friedman *et al* found that *there are seeds in the grape*: Instead of being spread all over the proton's volume, the electric charge seemed to be concentrated in a few point particles. This was the first *direct* evidence of the quarks as real physical objects. Moreover, when probed at high momenta, the quarks appeared to to be fairly independent from each other, quite contrary from their strong interactions in the non-relativistic quark model. To many theorists — especially Kurt Symanzik — this meant that the underlying theory of the strong force must be an asymptotically free theory.

Unfortunately, the only asymptotically free QFT known at that time was the unphysical $\lambda\Phi^4$ theory with a negative coupling $\lambda < 0$. Although Iosif Khriplovich have found the opposite-from-QED sign of charge renormalization in Yang–Mills theories back in 1969, but he did not connect this to the asymptotic freedom, so his work went unnoticed until much later. Then in 1972 Gerard 't Hooft calculated the beta-functions of non-abelian gauge theories and saw that many such theories do have $\beta < 0$ so they are asymptotically free. Immediately after that, 't Hooft himself and many of his European colleagues tried to come up with an AF non-abelian gauge theory of the strong force, but they did not make it because they did not believe in the colors of the quarks.⋆ So it took an extra year and 3 Americans — David Gross, Frank Wilczek, and (independently) Hugh Politzer — to discover the Quantum Chromodynamics (QCD) in 1973 and to verify that it is indeed asymptotically free.

⋆ Back then, there were two alternative solutions to the statistics problem of the non-relativistic quark model: The wave functions of baryons seem to be symmetric rather than antisymmetric in the combined positions, spins, and flavors of the 3 constituent quarks, so how does the baryon end up a fermion? One solution was the *parastatistics* — the modified Pauli principle that allows up to 3 quarks in the same quantum state, — while the other was to make quark ordinary fermions but to give them an extra degree of freedom — the color $i = 1, 2, 3$. Back in 1972, most European physicists did not like the invisible degrees of freedom like the color and preferred the parastatistics solution, while most American physicists thought parastatistics was BS and preferred the 3-color solution.

Specifically, a QCD-like theory with N_c quark colors (and hence the $SU(N_c)$ gauge group) and N_f quark flavors has one-loop beta-function

$$\beta_{1-\text{loop}}(g) \;=\; \frac{g^3}{48\pi^2}\times\left(2N_f^{\text{eff}}-11N_c\right) \tag{12}$$

where N_f^{eff} is the number of quark flavors with masses lighter than the relevant energy scale E. So as long as $N_f^{\text{eff}} < \frac{11}{2}N_c$, this beta-function is negative and the theory is asymptotically free. In particular, the real-life QCD has 3 colors and 6 flavors altogether, thus

$$2N_f^{\text{eff}} \;-\; 11N_c \;\leq\; 2N_f^{\text{total}} \;-\; 11N_c \;=\; 2\times 6-11\times 3 \;=\; -21 \;<\; 0, \tag{13}$$

so QCD is indeed asymptotically free.

Now let's solve the RGE for the QCD coupling g in the one-loop approximation. For simplicity, let's ignore the quark mass thresholds for a moment and let

$$\frac{dg}{d\log E} \;=\; \beta(g) \;\approx\; -\frac{Bg^3}{16\pi^2} \tag{14}$$

for a constant positive coefficient B. Then

$$B\times d\log E \;=\; -\frac{16\pi^2}{g^3}\,dg \;=\; d\left(+\frac{8\pi^2}{g^2}\;=\;+\frac{2\pi}{\alpha}\right) \tag{15}$$

and consequently

$$\frac{2\pi}{\alpha(E)} \;=\; \text{const} \;+\; B\times\log E. \tag{16}$$

Thus, if we happen to know the value $\alpha(E_1)$ of the QCD coupling at some energy scale E_1 (for example, the mass of the Z^0 weak gauge boson), then at all other energy scales

$$\frac{2\pi}{\alpha(E)} \;=\; \frac{2\pi}{\alpha(E_1)} \;+\; B\times\log\frac{E}{E_1}\,. \tag{17}$$

Graphically, we have

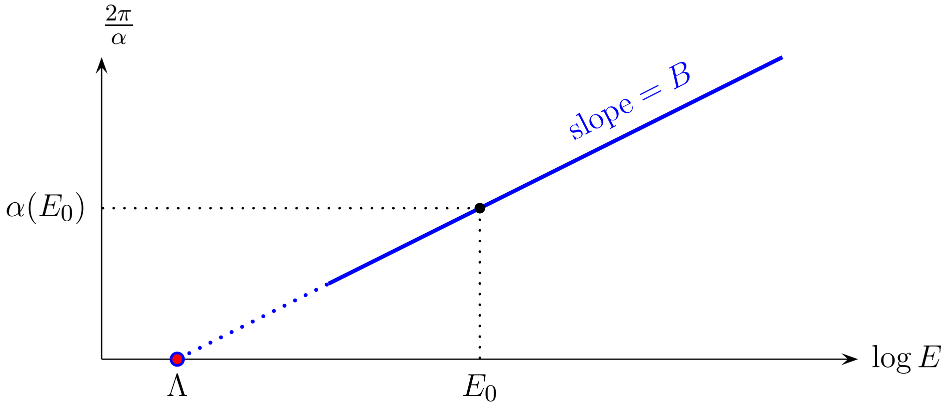

(18)

and hence

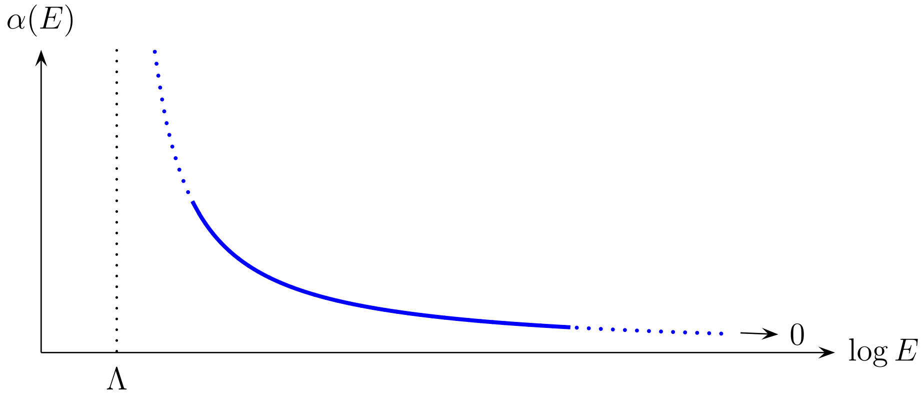

(19)

On the right side of this plot we see the asymptotic freedom — the QCD coupling $\alpha(E)$ becomes weaker and weaker with the increasing energy scale. But on the left side of the same plot we see the infrared price of the asymptotic freedom: at lower energy scales — *i.e.*, at longer distances — the coupling becomes stronger and stronger, until it eventually blows up some scale Λ AKA Λ_{QCD}. Of course, the one-loop approximation becomes invalid for the IR-strong coupling, so we would need a higher-loop and ultimately non-perturbative calculations to find whether $g(E)$ actually blows up for $E \to \Lambda$ or merely becomes non-perturbatively strong. But either way, we cannot use the perturbation theory at low energies $E \lesssim \Lambda$; instead, we need to use some non-perturbative techniques such as lattice gauge theory or holographic gauge/gravity duality.

Phenomenologically, QCD has two major non-perturbative effects at the low-energy scales $E \sim \Lambda$: the *confinement*, and the *chiral symmetry breaking*. I have discussed the χSB in class back in November, and I shall explain the mechanism of confinement on some other occasion. For the moment, let me simply describe its consequences. Basically, while the forces between the fundamental quanta of QCD — the quarks, the antiquarks, and the gluons — are Coulomb-like at short distances, but at longer distances the forces do not vanish as $1/r^2$ but asymptote to non-zero values,

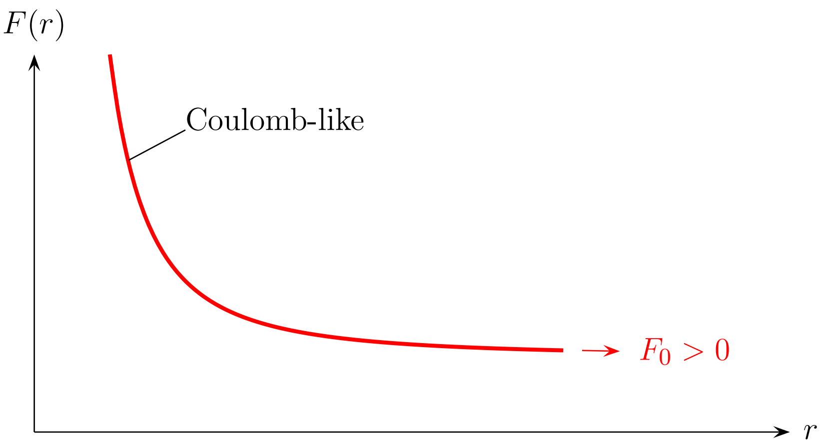

(20)

In particular, for a quark-antiquark pair, the long-distance force is $F_0 \approx 150$ kN ≈ 15 tonnes.

Because of this long-distance force, the quarks, the antiquarks, and the gluons never show up as standalone particles but are confined to color-singlet bound states, hence the name 'confinement'. Instead, the particle states of QCD are the color-singlet bound states:

- The $q\bar{q}$ mesons, the qqq baryons, the $\bar{q}\bar{q}\bar{q}$ antibaryons, collectively called the hadrons.
- The gg, ggg, *etc.*, glueballs.
- The exotics $q\bar{q}g$, $qq\bar{q}\bar{q}$, $qqqq\bar{q}$, *etc.*, *etc.*

Because of confinement and other non-perturbative effects at low momenta, QCD does not have a low-energy limit α_0 of its running coupling $\alpha(E)$. Alas, in this aspect, QCD is quite different from QED or the $\lambda\Phi^4$ theory: while in those theories we may start with the low-energy α_0 or λ_0 and use it as the initial condition for the renormalization group equations, in QCD we have to start by measuring the running coupling α_1 at some high-enough energy scale $E_1 \gg \Lambda$, and then follow the RGE solution to other energies, both higher and lower than the E_1. At the one-loop level, this solution is simply

$$\frac{2\pi}{\alpha(E)} \;=\; \frac{2\pi}{\alpha_1} \;+\; B\times\log\frac{E}{E_1}\,, \tag{17}$$

but at higher loop orders it becomes more complicated.

Instead of specifying the α_1 coupling in eq. (17) — which makes sense only in the context of a known initial energy scale E_1 (for example, $E_1 = M_Z$), — we may rewrite the RHS of that formula as

$$\frac{2\pi}{\alpha(E)} \;=\; B\times\log\frac{E}{\Lambda} \tag{21}$$

$$\text{where } \Lambda \;=\; E_1\times\exp\left(-\frac{2\pi}{B\alpha_1}\right), \tag{22}$$

and then specify just the Λ as the initial condition for the RGE. Since the α_1 coupling is dimensionless while Λ has dimension of energy, this change of specification is called the *dimensional transmutation.*

However, the precise definition of $\Lambda_{\rm QCD}$ in eq. (21) involve two important subtleties. First, there are different renormalization schemes for the precise definition of the running coupling $\alpha(E)$. In general, two couplings $\alpha_1(E)$ and $\alpha_2(E)$ at the same energy scale E but according to 2 different renormalization schemes differ by

$$\alpha_2(E) \;-\; \alpha_1(E) \;=\; O(\alpha^2(E)), \tag{23}$$

hence

$$\frac{2\pi}{\alpha_2(E)} \;-\; \frac{2\pi}{\alpha_1(E)} \;=\; O(1) \tag{24}$$

and therefore

$$\Lambda_2 \;=\; \Lambda_1\times\bigl(O(1)\text{ numeric constant}\bigr). \tag{25}$$

For example, the Λ's for the MS and the $\overline{\rm MS}$ renormalization schemes are related as

$$\Lambda[{\rm MS}] \;=\; \Lambda[\overline{\rm MS}]\times\left(\sqrt{\frac{4\pi}{e^{\gamma_E}}}\approx 2.66\right). \tag{26}$$

Second, the B coefficient in eq. (21) changes when the energy scale E crosses a quark mass threshold at m_c, m_b, or m_t. Indeed,

$$B = \frac{11}{3}N_c - \frac{2}{3}N_f^{\text{eff}} \tag{27}$$

where N_f^{eff} is the number of quark flavors with masses lighter than E. Thus,

$$\begin{array}{lrl} \text{for} & E > m_t \approx 175 \text{ GEV} & b = 7, \\ \text{for} & m_t > E > m_b \approx 4.5 \text{ GeV} & b = \frac{23}{3}, \\ \text{for} & m_b > E > m_c \approx 1.5 \text{ GeV} & b = \frac{25}{3}, \\ \text{for} & E < m_c & b = 9. \end{array} \tag{28}$$

Note: the light quark flavors u, d, s have masses smaller than Λ_{QCD}, so they do not lead to B-changing thresholds. But the heavy flavors c, b, t have masses in the perturbative range of $\alpha(E)$, so they do lead to thresholds in the RGE for the QCD coupling.

With all these effects in mind, let me finally tell you the actual Λ_{QCD} and plot the running QCD coupling $\alpha(E)$. The experimental measurements of α_{QCD} at high energies are usually renormalized to $E_1 = M_Z \approx 91$ GeV in the $\overline{\text{MS}}$ regularization scheme,

$$\alpha_{\text{QCD}}(M_Z)[\overline{\text{MS}}] = 0.1179 \pm 0.0010. \tag{29}$$

This further translates to the Λ of the five-flavor QCD (since the sixth flavor is heavier than M_Z)

$$\Lambda_5[\overline{\text{MS}}] = M_Z \times \exp\left(-\frac{6\pi}{23\alpha(M_Z)}\right) \approx 85 \text{ MeV}. \tag{30}$$

However, Λ_{QCD} is usually quoted in a slightly different regularization scheme MS as

$$\Lambda_5[\text{MS}] \approx 225 \text{ MeV}. \tag{31}$$

Also, below the bottom quark's mass — and then again below the charm quark's mass, —

the effective number of flavors drops from 5 to 4 to 3, so the 3-flavor lowish-energy QCD has

$$\Lambda_3[\overline{\mathrm{MS}}] \;\approx\; 330\ \mathrm{MeV}.$$

On the other hand, the high-energy 6-flavor QCD at $E > m_t$ has

$$\Lambda_6[\overline{\mathrm{MS}}] \;\approx\; 120\ \mathrm{MeV}. \tag{32}$$

And with all these data in mind, here is the plot of the running QCD coupling:

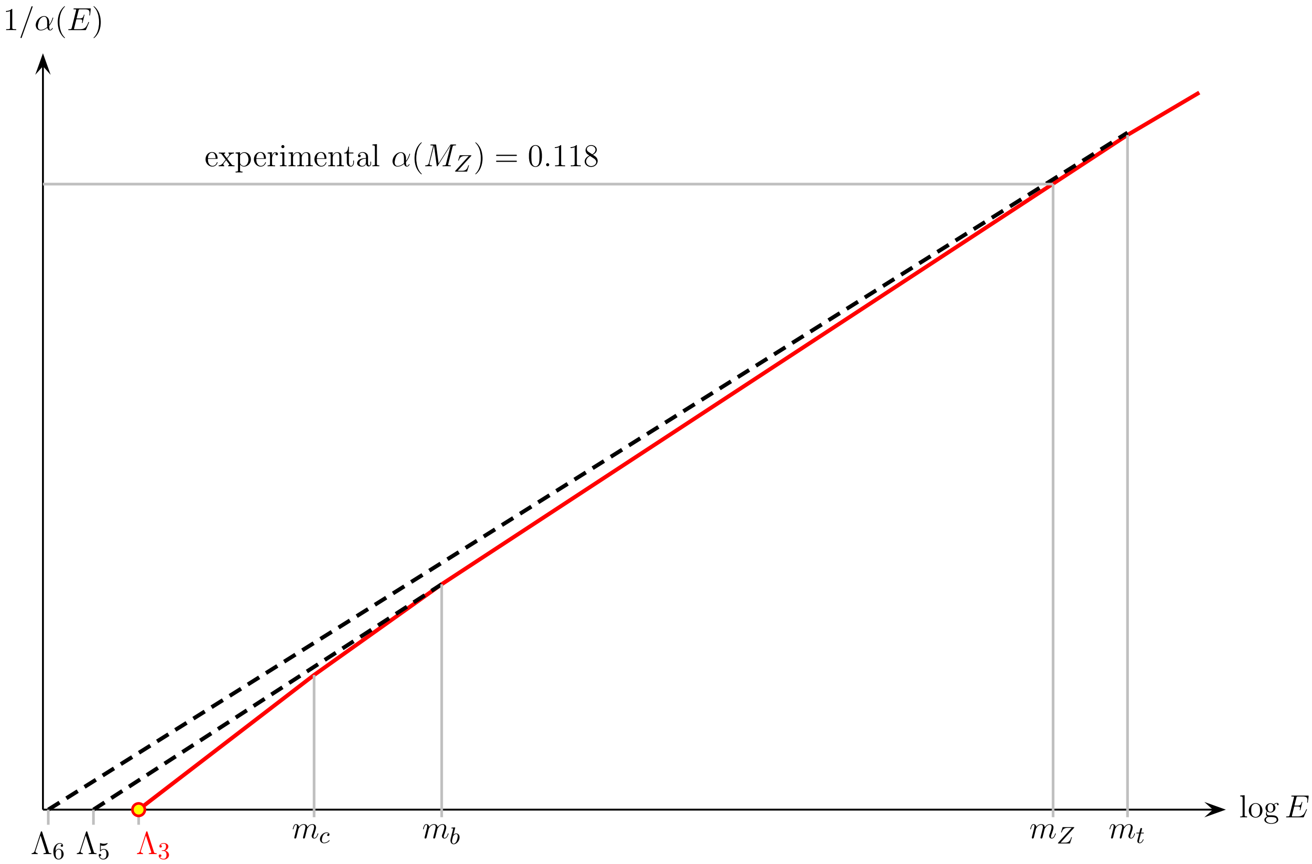

Fixed Points of the RG Flow

Thus far we looked at $\beta(g)$ functions that are either positive at all g or negative at all g. But now suppose the beta function changes sign at some critical value g^* of the coupling g. That is, either (A) $\beta(g)$ is positive for $g < g^*$ but negative for $g > g^*$ or (B) the other way around, $\beta(g < g^*) < 0$ but $\beta(g > g^*) > 0$:

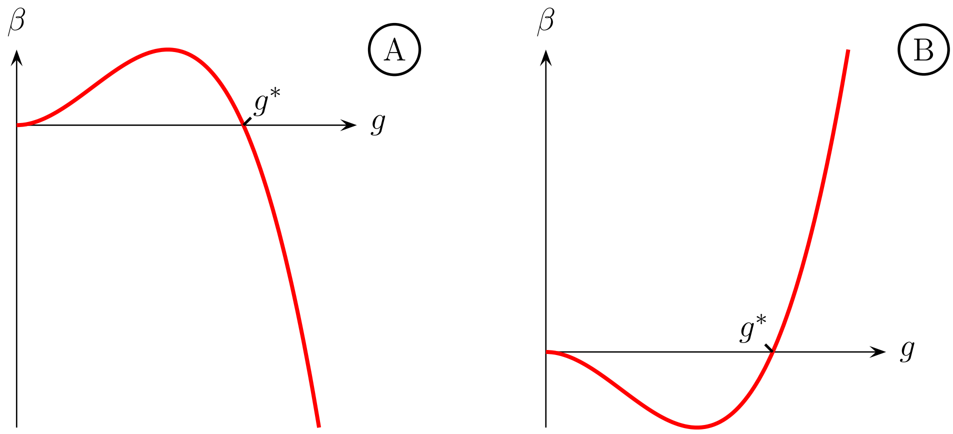

(33)

Either way, at $g = g^*$, the beta function happens to vanish.

Now suppose at some starting energy scale E_1, the running coupling happens to be equal to the g^*, $g(E_1) = g^*$. Then at that point

$$\left.\frac{dg(E)}{d\log E}\right|_{E_1} \;=\; \beta(g(E_1) = g^*) \;=\; 0, \tag{34}$$

and consequently solving the RGE equation for the $g(E)$ yields the constant solution,

$$\forall E: \quad g(E) \;\equiv\; g^* \;=\; \text{const}. \tag{35}$$

Consequently — assuming g is the only running coupling of the theory and all the particles are massless — we have a scale invariant quantum theory. That is, it's invariant under scale transforms (AKA dilatations) which act as

$$\begin{aligned} x'_\mu \;&=\; C \times x_\mu \quad \text{for a constant } C \neq 0, \\ E' \;&=\; C^{-1} \times E, \\ \Phi'(x') \;&=\; C^{-\Delta} \times \Phi(x) \\ \text{where } \Delta \;&=\; 1 + \gamma^* \;=\; 1 + \gamma(g = g^*),\ \text{same } \forall E, \end{aligned} \tag{36}$$

and likewise for spinor and vector fields, if any. Even the composite operators — like $\Phi^2(x)$

or $\overline{\Psi}(x)\Psi(x)$ in QED — scale like fixed powers of E and hence C:

$$\hat{\mathcal{O}}'(x') \;=\; C^{-\Delta_{\mathcal{O}}} \times \hat{\mathcal{O}}(x) \tag{37}$$

for a constant dimension

$$\Delta_{\mathcal{O}} \;=\; \Delta_{\mathcal{O}}^{\text{canonical}} \;+\; E\text{-independent quantum correction.} \tag{38}$$

Note: many field theories with massless fields — for example, QED with massless electrons — are *classically* invariant under scale transforms, but the quantum theories lose this scale invariance due to non-zero beta-functions and hence energy-dependent couplings $g(E)$. Only of the beta-function vanishes for some value g^* of the coupling, and if the theory happens to have that particular value of the coupling, only then the theory is truly scale invariant at the quantum level.

Moreover, for a relativistic quantum field theory, the scale invariance and Poincare symmetry (translations plus Lorentz) *usually* combine to the *conformal symmetry.* To be precise, in $d = 2$ spacetime dimensions there is a theorem saying that a scale-invariant and Poincare-invariant QFT must be conformally invariant. In $d = 4$ dimensions, there is no such symmetry, and there are counterexamples of some weird QFTs with Poincare and scale symmetries but no conformal symmetry. But these counterexamples are quite weird; for the more conventional QFTs of scalar, spinor, and vector fields, relativity plus scale invariance almost certainly means conformal symmetry.

There many books written on the conformal field theories (CFTs), *i.e.* conformally symmetric quantum field theories. The $d = 1 + 1$ dimensional CFTs are particularly important in string theory — where they live on the string's worldsheet. But the higher-dimensional CFTs are also very important, both in condensed matter theory (where they describe the critical phenomena) and in relativistic QFT. I wish I could explore CFTs in our class, but alas the time is too short, and the worthy subjects are too many, so let's move on.

Or at least, let's move on off a fixed point g^* to a different coupling $g \neq g^*$. That is, suppose at some starting point E_1 we have $g(E_1) \neq g$, and let's see what happens to the running coupling $g(E)$ at other energies. The answer here depends on whether $\beta(g)$ is positive for $g < g^*$ and negative for $g > g^*$ or the other way around, *cf.* 2 plots on figure (33).

Let's start with the case (A):

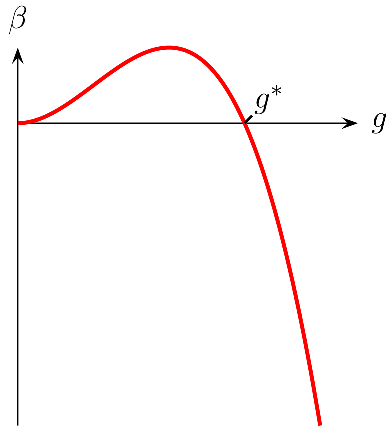

(39)

In this case, for $g < g*$, $\beta(g)$ is positive so $g(E)$ increases with the energy. On the other hand, for $g > g^7$, he $\beta(g)$ is negative so $g(E)$ decreases with the energy. Either way, as the energy E increases, the running coupling $g(E)$ gets closer to the fixed point g^*. In other words, in the UV direction of $\log E \to +\infty$, the running coupling $g(E)$ flows towards the fixed point g^*. Here is a typical plot of RG flow trajectories starting with different initial $g(E_1)$ and flowing towards the fixed point:

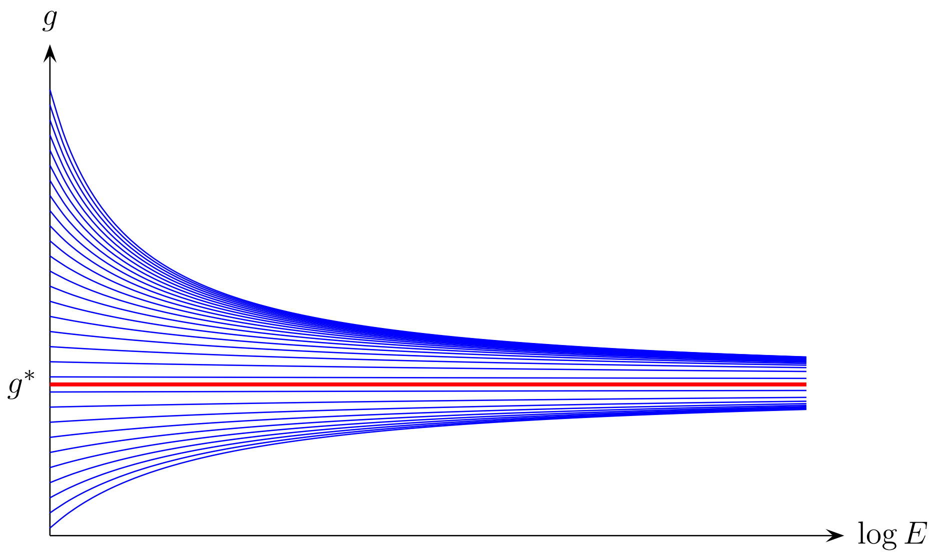

(40)

Thus, regardless of the 'initial' low-energy coupling $g(E_1)$, in the extreme UV limit the coupling asymptotes to the fixed point, and we end up with a scale-invariant theory. Consequently, the fixed points like in figure (39) — *i.e.*, with a negative derivative

$$\beta' = \left.\frac{d\beta(g)}{dg}\right|_{g^*} < 0, \tag{41}$$

— are called *UV stable*. And the derivative β' here governs the rate at which the running coupling asymptotes to the fixed point. Indeed, suppose $g(E)$ is already close to g^*, then

$$\beta(g) \;\approx\; \beta' \times (g - g^*), \tag{42}$$

hence

$$d\log E \;=\; \frac{dg}{\beta(g)} \;\approx\; \frac{1}{\beta'}\,\frac{dg}{g-g^*} \;=\; \frac{1}{\beta'}\,d\log(g-g^*), \tag{43}$$

and therefore

$$g(E) \;-\; g^* \;=\; \text{const} \times E^{\text{negative}\,\beta'} \;\xrightarrow[E\to\infty]{}\; 0. \tag{44}$$

The flip side of a UV-stable fixed point is that it's unstable when the energy scale flows in the IR direction. That is, if at some initial energy E_1 the coupling $g(E_1)$ is less than the fixed point, then at much lower energies $E \ll E_1$, the running coupling gets smaller and smaller, and eventually asymptotes to zero. On the other hand, if $g(E_1) > g^*$, then at much lower energies $g(E)$ grows larger and larger, until it eventually blows up. Of course, this behavior assumes a massless theory, while in a massive theory, the RG flow in the IR direction stops at $E \simeq M$.

Now consider case (B):

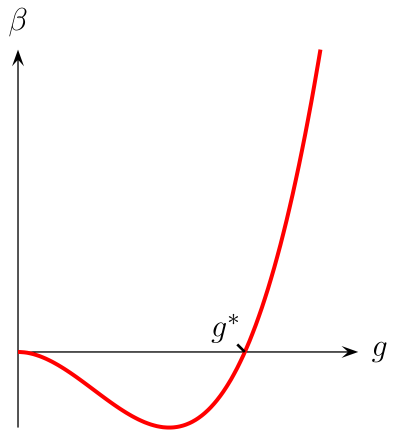

(45)

This time, if we start with a $g < g^*$, then $g(E)$ gets smaller with the increasing energy, and eventually asymptotes to zero for $E \to \infty$. This is asymptotic freedom. However, if we start with $g > g^*$, then $g(E)$ gets larger at the higher energies, and eventually blows up in a

Landau pole. Either way, the RG flow in the UV direction moves $g(E)$ away from the fixed point:

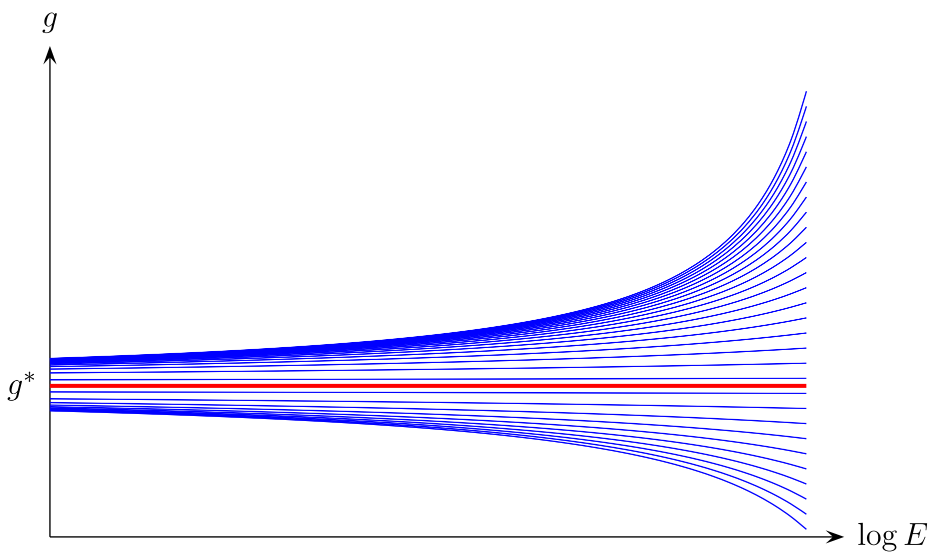

(46)

On the other hand, the RG flow in the IR direction brings $g(E)$ closer and closer to the fixed point g^*, regardless of whether we start with $g > g^*$ or $g < g^*$. Thus, in case (B) — the fixed point with a positive derivative β' (at $g = g^*$) — are *IR stable.* And once the coupling $g(E)$ gets close to g^*, it asymptotes to g^* according to

$$g(E) \;-\; g^* \;=\; \text{const} \times E^{\text{positive}\,\beta'} \;\xrightarrow[E\to 0]{}\; 0. \tag{47}$$

Theories with fixed points like these — and with no masses to stop the RG flow to the deep IR — do not have scale invariance at short distances, but their long-distance behavior is scale invariant and can be described by an effective CFT. Indeed, may interesting CFTs obtain from the deep IR limits of the non-conformal QFTs with non-trivial fixed points. So let me present a couple of examples: (1) Wilson's critical point in condensed matter in $D < 4$ dimensions, and (2) Banks–Zaks conformal window of QCD.

Wilson's Critical Point in $D < 4$ dimensions.

Consider the $\lambda\Phi^4$ theory in $D < 4$ dimensions. In condensed matter context, $D = 3$, $\Phi(x)$ is the magnetization field along some preferred direction, and its mass^2 is tuned to zero by adjusting the temperature and/or the pressure to the critical point. But for our purposes, we don't care about the physical meaning of the Φ field and how is mass ^{2} is tuned to zero, as long as it is so tuned so we may follow the RG flow all the way to the deepest infrared. Also, we allow for a generic non-integer dimension D as long as $D < 4$, in particular for the $D = 4 - 2\epsilon$.

In $D < 4$ dimensions of space, the Φ^4 coupling λ has dimensionality E^{4-D}, so the proper dimensionless running coupling is

$$\hat{\lambda}(E) \;=\; \lambda(E) \times E^{D-4}, \tag{48}$$

and the corresponding beta-function is

$$\begin{aligned} \hat{\beta}(\hat{\lambda}) \;&=\; (D-4) \times \hat{\lambda} \;+\; \beta_{4d}(\hat{\lambda}) \\ &=\; (D-4) \times \hat{\lambda} \;+\; \frac{3\hat{\lambda}^2}{16\pi^2} \;-\; \frac{17\hat{\lambda}^3}{6(4\pi)^4} \;+\; \cdots. \end{aligned} \tag{49}$$

Viewing the bottom line here as a power series in $\hat{\lambda}$, we see that the leading term is negative while the first subleading term is positive, so at small $\hat{\lambda}$, this beta-function indeed behaves as in case (B):

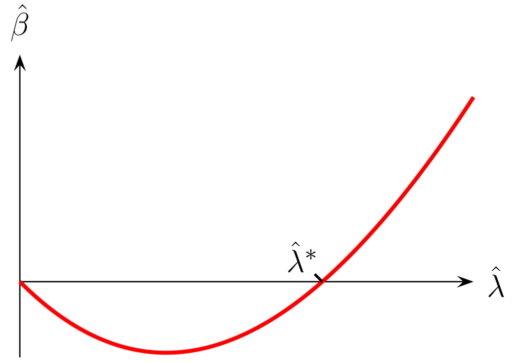

(50)

As to the zero $\hat{\lambda}^*$ of this beta-function, it obtains by solving

$$(4-D) \;=\; \frac{\beta_{4d}(\hat{\lambda}^*)}{\hat{\lambda}^*} \;=\; +3\frac{\hat{\lambda}^*}{16\pi^2} \;-\; \frac{17}{6}\left(\frac{\hat{\lambda}^*}{16\pi^2}\right)^2 \;+\; \cdots. \tag{51}$$

For $D = 4 - 2\epsilon$ — and small ϵ — the solution is small,

$$\frac{\hat{\lambda}^*}{16\pi^2} \;=\; \frac{2}{3}\epsilon \;+\; \frac{34}{81}\epsilon^2 \;+\; \cdots, \tag{52}$$

and we may trust the weak-coupling perturbation theory. But extrapolating this solution to the condensed-matter case of $D=3$ yields

$$\frac{\hat{\lambda}^*}{16\pi^2} = \frac{1}{3} + \frac{17}{162} + \cdots, \tag{53}$$

which looks marginal: weak enough to expect the leading-order perturbative results to be in the right ballpark, but too strong to trust the perturbation theory to be more accurate than that. In practice though, the anomalous dimensions and other critical exponents calculated to the leading order in $\hat{\lambda}$ for $(\hat{\lambda}/16\pi^2) = \frac{1}{3}$ — as in the leading order of eq. (53) — seem to be fairly close to the experimental results.

Conformal Window of QCD

Consider a QCD-like theory in $D=4$ dimensions with N_c colors and N_f exactly massless quark flavors. The 2-loop beta-function of this theory has been calculated back in 1970s,

$$\beta(g) = b_1 \times \frac{g^3}{16\pi^2} + b_2 \times \frac{g^5}{(4\pi)^4} + \cdots, \tag{54}$$

$$\text{for } b_1 = \frac{2}{3}N_f - \frac{11}{3}N_c\,, \tag{55}$$

$$\text{and } b_2 = \frac{13}{3}N_f N_c - \frac{N_f}{N_c} - \frac{34}{3}N_c^2\,. \tag{56}$$

Thus, for large numbers of colors and flavors, and the flavor-to-color ratio N_f/N_c in the range

$$\frac{11}{2} > \frac{N_f}{N_c} > \frac{34}{13} \tag{57}$$

we have $b_1 < 0$ but $b_2 > 0$. Consequently, the 2-loop beta function looks like case (B):

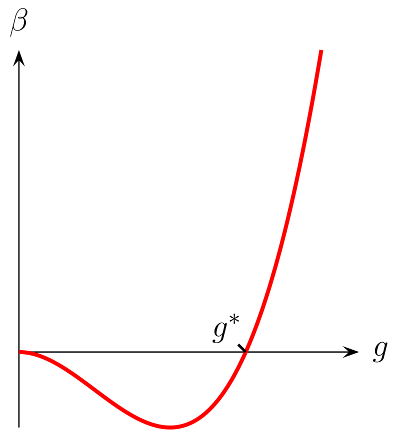

$$\text{for } \frac{g^{*2}}{16\pi^2} = \frac{-b_1}{b_2}\,. \tag{58}$$

But since this calculation is based on truncating the QCD beta function to the first two loop orders, it is trustworthy only if it happens to yield a weak fixed coupling g^*, or rather a weak 't Hoof coupling

$$\lambda^* \stackrel{\text{def}}{=} N_c \times \frac{{g^*}^2}{16\pi^2} \ll 1. \tag{59}$$

But alas, for generic flavor to color ratios within the range (57), we end up with

$$\lambda^* = \frac{(-b_1)N_c}{b_2} = O(1), \tag{60}$$

so our calculation is unreliable: Not only we cannot trust the value of the fixed coupling λ^*, but we cannot even be sure that the beta-function actually has a zero at come coupling.

In 1982, Banks and Zaks solved this problem by focusing on the upper edge of the range (57). That is, let's take the limit

$$N_c \to \infty, \quad N_f \to \infty, \quad \text{but } \Delta \stackrel{\text{def}}{=} 11N_c - 2N_f \text{ is positive and small, } \Delta \ll N_c\,. \tag{61}$$

In this limit,

$$\begin{aligned} -b_1 &= +\frac{1}{3}\Delta, \\ \text{while } b_2 &\approx +\frac{25}{2}N_c^2, \end{aligned} \tag{62}$$

hence

$$\lambda^* \approx \frac{2}{75} \times \frac{\Delta}{N_c} \ll 1. \tag{63}$$

Thus, in the Banks–Zaks limit, QCD does have a weakly-coupled IR-stable fixed point of the RG flow. And if all the quark flavors are exactly massless, then the deep IR limit of this theory is a weakly-coupled conformal field theory.

Outside of the Banks–Zaks limit, the deep IR limit of QCD-like theories with massless quarks depends on the flavor-to-color ratio:

⋆ For $(N_f/N_c) > \frac{11}{2}$, QCD is in the *non-abelian Coulomb phase*. In this regime $\beta(g) > 0$ even for weak couplings, so there is no asymptotic freedom. On the other hand, at low energies the running coupling becomes weaker and weaker, until in the deep IR the quarks and the gluons become almost-free massless particles with rather weak Coulomb forces between them. Or rather, non-abelian versions of the Coulomb forces, hence the name of this phase.

* ⋆ The $\frac{11}{2} > (N_f/N_c) >$ about 4 range is the so-called *conformal window.* In this regime, the beta-function has a IR-stable zero, so the deep IR limit of QCD is a conformal field theory of some kind. In the Banks–Zaks corner of this range, this CFT is weakly coupled, but through the rest of the conformal window it becomes strongly coupled, $\lambda^* = O(1)$, and we cannot use the perturbation theory to calculate the scaling dimensions of various operators. Although one might be able to use some non-perturbative techniques, such as lattice gauge theory. Indeed, it was the lattice gauge theory that gave us the approximate lower end of the conformal window.

* ⋆ For $(N_f/N_c) <$ about 4, QCD is in the *confining phase*, just like the real-life QCD. In this phase $\beta(g) < 0$ at all couplings, so in the IR direction the running coupling gets stronger and stronger until it blows up at $E \sim \Lambda_{\text{QCD}}$. Below this energy scale, the quarks and the gluons become confined and do not appear as standalone particles; instead, the particle spectrum is made from the color-singlet combinations of quarks and gluons, such as mesons, baryons, or glueballs. Almost all of these composite particles are massive — with masses $O(\Lambda_{\text{QCD}})$ — except for the Goldstone bosons of the spontaneously broken chiral symmetry $SU(N_f)_L \times SU(N_f)_R \to SU(N_f)_V$. But while the Goldstone bosons are massless, their interactions with each other are proportional to their momenta, so in the low-energy limit these bosons become free. So ultimately, the deep IR limit of QCD in the confining phase is the free theory of $N_f^2 - 1$ Goldstone bosons.

RG Flows for Multiple Couplings

Up to now we have focused on QFTs with a single running coupling $g(E)$ or $\alpha(E)$ or $\lambda(E)$. But many QFTs have multiple couplings: For example, the Standard Model has 3 gauge couplings $\alpha_1(E)$, $\alpha_2(E)$, $\alpha_3(E)$, the Higgs scalar's selfcoupling $\lambda(E)$, and a truckload of Yukawa couplings of the Higgs to the quarks and the leptons. For such theories, each coupling has its own renormalization group equation

$$\frac{dg_i(E)}{d\log E} \;=\; \beta_i(g_1(E),\ldots,g_N(E)), \tag{64}$$

where each beta-function depends on all the couplings of the theory. Thus, the RGEs are a system of coupled differential equations, and are generally much harder to solve than the RGE for a single coupling.

As a pedagogical example, consider the Yukawa theory

$$\mathcal{L}_{\rm phys} = \overline{\Psi}(i\partial\!\!\!/ - M)\Psi + \frac{1}{2}(\partial_\mu\Phi)^2 - \frac{M^2}{2}\Phi^2 - ig\Phi\times\overline{\Psi}\gamma^5\Psi - \frac{\lambda}{24}\Phi^4 \tag{65}$$

with 2 running couplings $g(E)$ and $\lambda(E)$, thus 2 coupled RGEs

$$\frac{dg(E)}{d\log E} = \beta_g(g(E),\lambda(E)) \quad \text{and} \quad \frac{d\lambda(E)}{d\log E} = \beta_\lambda(g(E),\lambda(E)). \tag{66}$$

In my previous set of notes on the renormalization group I have calculated the beta-functions here to the 1-loop order:

$$\beta_g^{\rm 1\,loop} = \frac{5g^3}{16\pi^2}\,, \tag{67}$$

$$\beta_\lambda^{\rm 1\,loop} = \frac{3\lambda^2 + 8\lambda g^2 - 48g^4}{16\pi^2}\,, \tag{68}$$

so let's solve the eqs. (66) for these beta-functions.

Since $\beta_g^{\rm 1\,loop}(g)$ is independent of λ, we may solve the one-loop RGE for the Yukawa coupling independently of the $\lambda(E)$:

$$\frac{dg}{d\log E} = \frac{5g^3}{16\pi^2} \implies d\log E = \frac{dg}{\beta_g} = \frac{16\pi^2\,dg}{5g^3} = d\left(\frac{-8\pi^2}{5g^2}\right), \tag{69}$$

hence

$$\frac{8\pi^2}{g^2(E)} = \frac{8\pi^2}{g^2(E_0)} - 5\log\frac{E}{E_0}\,. \tag{70}$$

Graphically,

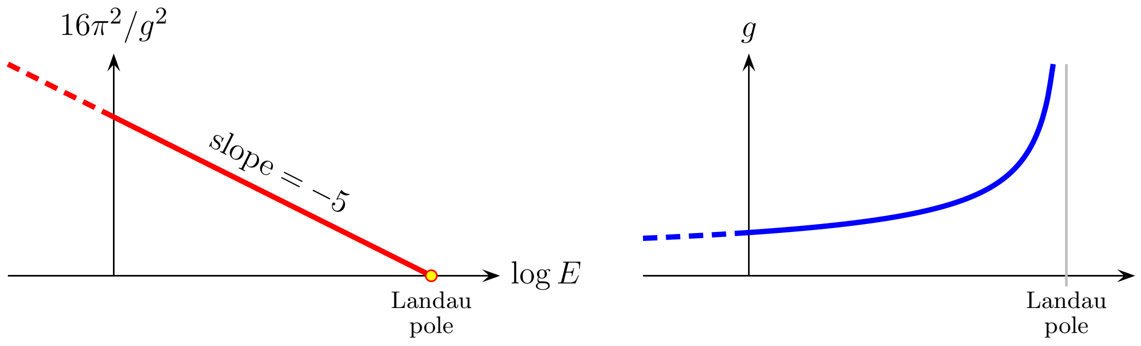

(71)

We see that similar to QED or to the $\lambda\phi^4$ theory, the Yukawa coupling keeps increasing with energy, and eventually at some very high energy hits a Landau pole. In the other hand, in the IR direction of the RG flow, the Yukawa coupling gets weaker and weaker until this RG flow is stopped by the scalar's mass or the fermion's mass. But if both masses happen to vanish, then the Yukawa coupling keeps getting weaker, and in the extreme IR limit the fermions become free.

The RG flow of the 4-scalar coupling $\lambda(E)$ is more complicated since β_λ depends on both couplings λ and g. To simplify solving the RGE for the $\lambda(E)$, we shall first focus on the *RG flow trajectory through the coupling space* (g^2, λ) — that is, we shall first calculate λ as a function of g^2 — and then plug in the energy-dependence of the $g^2(E)$ according to eq. (70). To get a differential equation for the $\lambda(g^2)$, we start by dividing the RGE for λ by the RGE for g^2, thus

$$\frac{d\lambda(E)}{dg^2(E)} = \frac{d\lambda}{d\log E} \Big/ \frac{2g\,dg}{d\log E} = \frac{\beta_\lambda}{2g\beta_g} = \frac{3\lambda^2 + 8\lambda g^2 - 48g^4}{10g^4}. \tag{72}$$

Next, we take the coupling ratio λ/g^2 to be a function of g^2, which in turn depends on the energy, thus

$$\frac{\lambda(E)}{g^2(E)} = X(g^2(E)), \tag{73}$$

and rewrite eq. (72) as a first-order differential equation for X: On one hand

$$\frac{d\lambda}{d(g^2)} = \frac{d}{d(g^2)}\big(\lambda = g^2 \times X(g^2)\big) = X + g^2 \times \frac{dX}{d(g^2)} = X + \frac{dX}{d\log g^2}, \tag{74}$$

while on the other hand eq. (72) becomes

$$\frac{d\lambda}{d(g^2)} = \frac{3X^2 + 8X - 48}{10}, \tag{75}$$

hence

$$\begin{aligned} X + \frac{dX}{d\log g^2} &= \frac{3X^2 + 8X - 48}{10}, \\ \frac{dX}{d\log g^2} &= \frac{3X^2 - 2X - 48}{10}, \end{aligned} \tag{76}$$

and therefore

$$\frac{dX}{3X^2 - 2X - 48} = \frac{1}{10} d\log(g^2(E)). \tag{77}$$

Integrating the LHS here we get

$$\int \frac{dX}{3X^2 - 2X - 48} \;=\; \frac{1}{2\sqrt{145}} \log \frac{3X - 1 - \sqrt{145}}{3X - 1 + \sqrt{145}} \;+\; \text{const}, \tag{78}$$

hence

$$\begin{aligned} \log \frac{3X - 1 - \sqrt{145}}{3X - 1 + \sqrt{145}} \;&=\; \left(\frac{2\sqrt{145}}{10} = \sqrt{\frac{29}{5}} \right) \times \log(g^2(E)) \;+\; \text{const}, \\ \frac{3X - 1 - \sqrt{145}}{3X - 1 + \sqrt{145}} \;&=\; \text{const} \times \big(g^2(E)\big)^{\sqrt{29/5}}, \end{aligned} \tag{79}$$

and therefore

$$\frac{3\lambda(E) \;-\; (\sqrt{145}+1)g^2(E)}{3\lambda(E) \;+\; (\sqrt{145}-1)g^2(E)} \;=\; \text{const} \times \big(g^2(E)\big)^{\sqrt{29/5}}. \tag{80}$$

The overall constant factor on the RHS here follows from the initial conditions to the RGE, namely the coupling values λ_0 and g_0 at some reference energy E_0, thus

$$\frac{3\lambda(E) \;-\; (\sqrt{145}+1)g^2(E)}{3\lambda(E) \;+\; (\sqrt{145}-1)g^2(E)} \;=\; \frac{3\lambda_0 \;-\; (\sqrt{145}+1)g_0^2}{3\lambda_0 \;+\; (\sqrt{145}-1)g_0^2} \times \left(\frac{g^2(E)}{g_0^2}\right)^{\sqrt{29/5}}. \tag{81}$$

Physically, eq. (81) describes a *trajectory of the renormalization group flow through the (g^2, λ) coupling space*. Here is a plot of several such trajectories for different initial values of (g_0^2, λ_0):

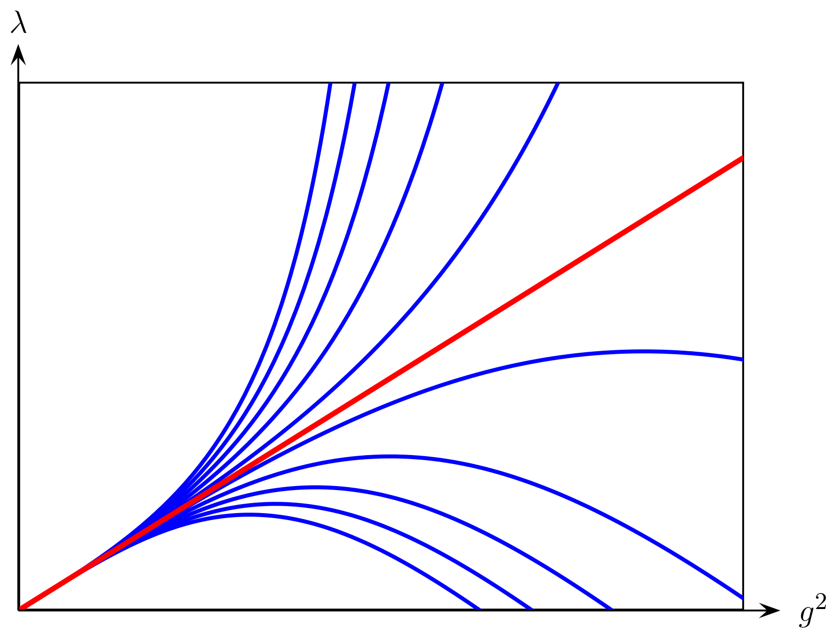

A few noteworthy features of these trajectories:

- Since $\beta_g > 0$ at all g, the UV-bound direction of these trajectories is to the right, while the IR-bound direction is to the left.
- In the IR direction, all trajectories converge to the attractor line (shown in red)

$$\lambda(E) \;=\; \frac{\sqrt{145}+1}{3} \times g^2(E). \tag{82}$$

  Note: this attractor line is not a line of fixed points: Once the couplings reach this line, they do not stop evolving with $\log(E)$ but continue to diminish with decreasing energy scale; they simply evolve in lock-step along the attractor line.
- In the UV direction, the trajectories spread out away from the red line.
  - ∗ If we start at some point above this line, then in the UV direction the λ/g^2 ratio keeps increasing until eventually $\lambda(g^2(E))$ hits a Landau pole. That is, it hits a Landau pole before the Landau pole of the $g^2(E)$ itself, assuming these Landau poles actually exist beyond the one-loop approximations to the β-functions.
  - ∗ On the other hand, if we start at some point below the red line, then the λ/g^2 ratio decreases in the UV direction until $\lambda(E)$ itself starts decreasing and eventually hits zero value. Beyond that point, a negative λ destabilizes the vacuum state of the theory due to unlimited-from-below scalar potential.
  - ∗ Similar to a Landau pole, a point where the scalar potential becomes unbounded from below acts as an upper limit on UV energy scales to which the original low-energy may be extrapolated. Beyond this limit we would need a different high-energy theory with more degrees of freedom. In other words, the original low-energy theory is *not* UV-complete.

⋆ ⋆ ⋆

Beyond the Yukawa theory, other QFTs with $n > 1$ independent coupling parameters generally have n coupled renormalization group equations:

$$\text{for each } i = 1, \ldots, n: \quad \frac{dg_i}{d\log E} \;=\; \beta_i(g_1, \ldots, g_n). \tag{83}$$

A common tool for solving such equations is to eliminate the $\log E$ variable — just like we did above for the Yukawa theory — and reduce the problem to a system of $n-1$ differential equations for the RG flow trajectory through the n-dimensional coupling space. Plotting the flow lines then reveals all kinds of interesting features, such as attractor lines, surfaces, *etc.*, bifurcation points (or lines, *etc.*), or even phase boundaries where the trajectories starting on two sides of a boundary end up in radically different places.

A particularly interesting features are the fixed points attracting all the trajectories — or at least all the trajectories starting within a particular *basin of attraction* — in either UV or IR direction. A theory that has such a fixed point becomes scale-invariant — and usually conformally invariant — in either extreme UV limit or extreme IR limit, depending on the type of a fixed point.

From the β-function point of view, a fixed point is a common zero of all n β-functions,

$$\text{all}\quad \beta_i(g_1^*,\ldots,g_n^*)\;=\;0. \tag{84}$$

Also, the derivative matrix

$$\mathcal{B}_{ij}\;=\;\left(\frac{\partial\beta_i}{\partial g_j}\right)_{(g_1^*,\ldots,g_n^*)} \tag{85}$$

determines the fixed point's type:

- If the matrix (85) is positive-definite (all eigenvalues are positive), then the fixed point is IR-stable. That is, the RG flow in the IR direction moves the couplings closer and closer to the fixed point.
- OOH, if the matrix (85) is negative-definite (all eigenvalues are negative), then the fixed point is UV stable. That is, the RG flow in the UV direction moves the couplings closer and closer to the fixed point.
- Finally, if the matrix (85) has both positive and negative eigenvalues, then the fixed point is unstable in both UV and IR directions: Either way, the RG flow moves some couplings (or coupling combinations) closer to the fixed point while other couplings or combinations move further away from it.